AIAA JOURNAL
Vol. 30, No. 6, June 1992

Computation of Saddle Point of Attachment

Ching-Mao Hung*
NASA Ames Research Center, Moffett Field, California 94035
Chao-Ho Sung†
David Taylor Research Center, Bethesda, Maryland 20084
and
Chung-Lung Chen‡
Rockwell International Science Center, Thousand Oaks, California 91360

Because of its reputed benign nature, the saddle point of attachment has not received critical attention to nearly the same extent as has the saddle point of separation. Recently, Visbal calculated low-speed flows around a cylinder mounted on a flat plate. Here, it was fully to be expected that the outermost critical point in the surface flow pattern ahead of the obstacle would be a saddle point of separation. The results indicated that the critical point was actually a saddle point of attachment, not separation. These results have brought to light a number of issues requiring additional study. In the present study, two numerical codes are used for a wide range of Mach numbers, Reynolds numbers, grid sizes, and numbers of grid points to confirm the existence of the saddle point of attachment in the flow before an obstacle. The computational results near the critical point are theoretically analyzed. The impact and significance of the saddle point of attachment to the interpretation of experimental surface flow patterns and the definitions of lines of separation and attachment are discussed. A line of oil accumulating from both sides can be either a line of separation or a line of attachment, depending on the characteristics of the saddle point.

I. Introduction

IT is commonly conceived that when a boundary layer encounters a bluff body protuberance (Fig. 1), the flow separates and rolls up to form a horseshoe vortex or a system of horseshoe vortices. This is a basic three-dimensional problem that has been studied experimentally for both compressible and incompressible flows over various geometries (e.g., Refs. 1-5); it has been simulated numerically for a blunt fin, wing juncture, and other geometries (e.g., Refs. 6-8).

Recently, Visbal[9] numerically studied low-speed laminar flows around a cylinder mounted on a flat plate. Figures 2a and 2b show the simulated oil-flow pattern on the flat plate and the streamline pattern in the plane of symmetry for a Reynolds number, based on cylinder diameter, $Re_D = 5 \times 10^2$. Figure 2a resembles an oil-flow pattern as regularly observed experimentally, and Visbal interpreted these results as the simplest separation pattern for a horseshoe vortex topology. As Re_D increased to 1.5×10^3, 2.6×10^3, 4×10^3, and 5.4×10^3, he observed that the flow topology evolved from a single primary horseshoe vortex to multiple horseshoe vortices.

However, a closer examination of Fig. 2b reveals that Visbal's result is quite different from the conventionally conceived flow structure of a horseshoe vortex. In Fig. 2b, there is indeed indication of a vortex, a spiral focus indicated as C, which is separated from the singular point S by a saddle point D. The fluid is flowing into the singular (critical) point S, not out; hence, the point S is an attachment point, not a separation point. Point S in Fig. 2a is a saddle point. Therefore, S is a saddle point of attachment, not a saddle point of separation. (Visbal[10] recently has realized that S is a saddle point of attachment.) Note that while the feature of a saddle point of separation is conventionally obtained in computations and experiments for various geometries and flow conditions, the potential presence of a saddle point of attachment for these geometries and flow conditions has not been suspected before. In general, as suggested by Lighthill[11] and Davey,[12] the presence of one or a series of saddle points of attachment was to be expected under flow conditions where attachment (e.g., at the leading edge of a wing or behind a backward-facing step) prevailed. Chapman[13] suggested that "the plane associated with a saddle point of attachment is not of great interest in fluid mechanics because its only special feature is bringing external flow to the surface." It is true that, although it may exist in nature and has been mentioned in other theoretical studies (e.g., Ref. 12), the role of the saddle point of attachment in fluid mechanics has never been made the central point of a computational or experimental study.

The objectives of the present study are threefold. The first is to confirm the existence of a saddle point of attachment in the flow before an obstacle. Two different numerical programs are employed to solve cases for various Mach numbers,

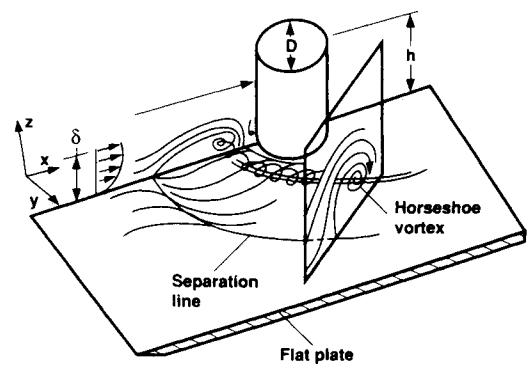

Fig. 1 Flow upstream of a cylinder mounted on a flat plate.

Received June 14, 1991; presented as Paper 91-1713 at the AIAA 22nd Fluid Dynamics, Plasma Dynamics, and Lasers Conference, Honolulu, HI, June 24-26, 1991; revision received Sept. 9, 1991; accepted for publication Sept. 13, 1991.

*Research Scientist. Associate Fellow AIAA.
†Engineering Staff Specialist.
‡Member Technical Staff. Member AIAA.

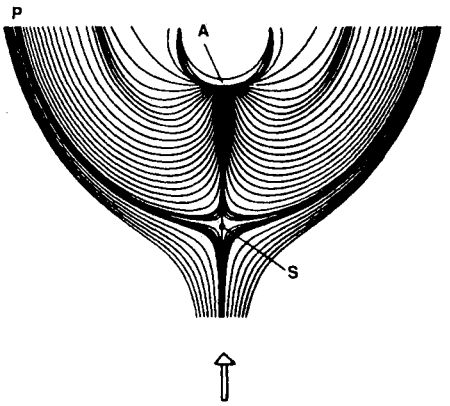

a) Simulated oil flow pattern on flat plate

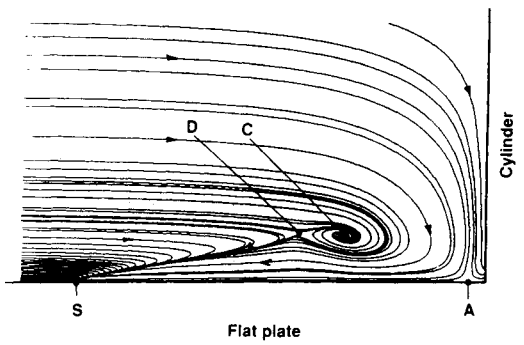

b) Streamline pattern on symmetry plane

Fig. 2 Computed results of Visbal for $Re_D = 5 \times 10^2$.

Reynolds numbers, grid sizes, and points. The second is to theoretically analyze the flow characteristics near the saddle point. Computational results are used to confirm the analysis. Cases for both saddle point of separation and saddle point of attachment are examined. The third is to address the significance of the saddle point of attachment to the construction of external flow structures, the interpretation of experimental surface oil-flow patterns, and the theoretical definition of three-dimensional flow separation. The definition of the line of separation is reassessed. A difficult problem is to establish an unambiguous definition of the line of attachment appropriate for general cases. Related issues will be addressed. In the present study, only steady flows, upstream of the obstacle, are considered, and most flows calculated are assumed laminar.

II. Numerical Solutions

As is generally known, computed results cannot be used to rigorously prove a physical concept or feature, but only to confirm, demonstrate, or illustrate its existence. In this respect, we tried to cover as wide a range as possible. Two different codes, both quite different from the code used by Visbal, were employed to obtain solutions for various flow conditions and grid systems. The first one (code A) is a code for incompressible flow developed by Sung.[7] An artificial compressibility concept is used and solutions are obtained by an explicit third-order Runge-Kutta method. The second one (code B) is a code for compressible flow developed by Chakravarthy et al.[15] in which an upwind scheme is used to solve the time-dependent Navier-Stokes equations. The cylinder has zero yaw, and so only a half of the cylinder is considered and a symmetry condition is imposed at the plane of symmetry. For code A, a half-O grid is used with the outer boundary located at 10 diam. Code B has the capability of multizone calculations; a half-O grid is combined with an H grid in the wake. It covers a domain similar to that of Visbal with different grid distribution. Details of numerical procedures for these two codes were presented and discussed in Refs. 7 and 15.

For both codes, at the outer boundary, a Blasius boundary-layer profile is prescribed. In contrast to Visbal's keeping the boundary-layer thickness constant, we allow the boundary-layer thickness to grow according to

$$\delta = \frac{5.0x}{\sqrt{Re_x}}$$

Note that, for a boundary layer of $\delta_0 = 0.1D$ at initial location x_0, over a distance of 20 diam downstream, the thickness of the boundary layer will grow, based on the above formula, about a factor of 10 for the case of $Re_D = 5 \times 10^2$, and a factor of 5.86 for the case of $Re_D = 1.5 \times 10^3$.

Many cases for a wide range of Reynolds numbers, grid sizes, and numbers of grid points have been calculated. In the code A calculations, systems of grid points vary from $25 \times 33 \times 33$ to $97 \times 97 \times 49$, with several different grid distributions. In the code B calculations, five cases of two Reynolds numbers and three Mach numbers have been studied. Figures 3–5 show typical computational results. Figures 3a–c are plots of the streamline pattern in the plane of symmetry and simu-

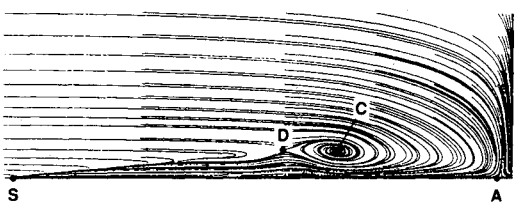

a) Particle traces in plane of symmetry

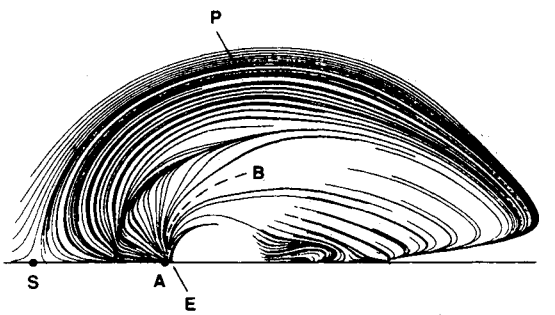

b) Simulated oil-flow pattern on the flat plate

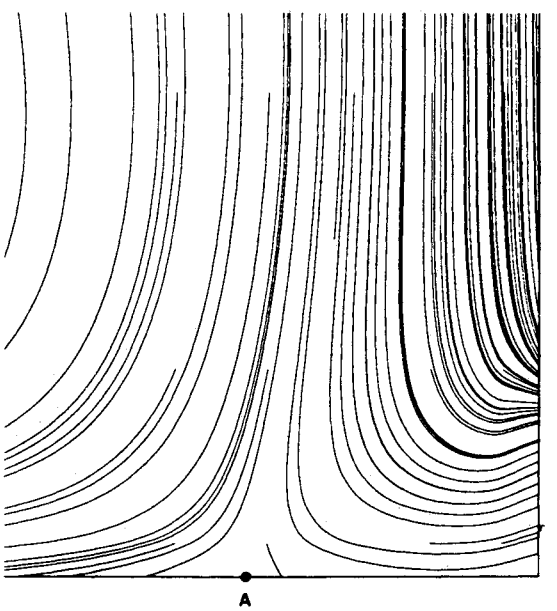

c) Detail of particle traces near the junction of cylinder and flat plate

Fig. 3 Computed results of an incompressible code for $Re_D = 1.5 \times 10^3$ with grid $49 \times 97 \times 33$.

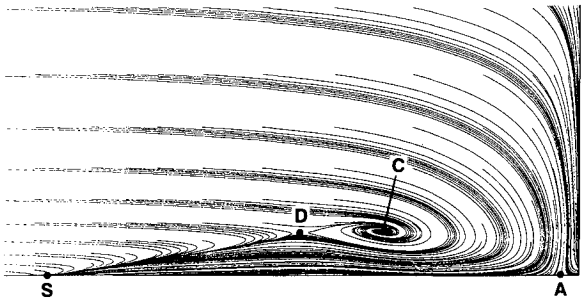

a) Particle traces in plane of symmetry

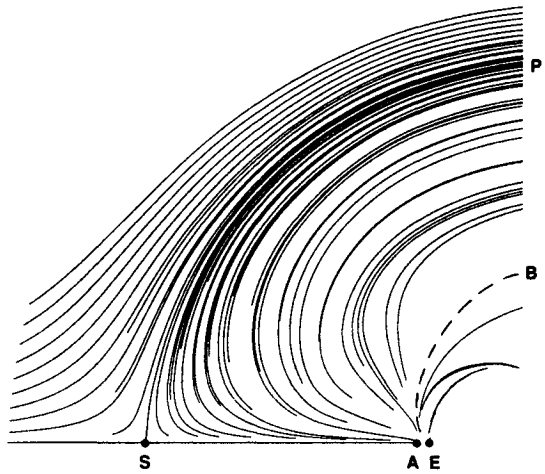

b) Simulated oil-flow pattern on the flat plate

Fig. 4 Results of a compressible code for $M_\infty = 0.2$, $Re_D = 5 \times 10^2$ with grid $103 \times 157 \times 35$.

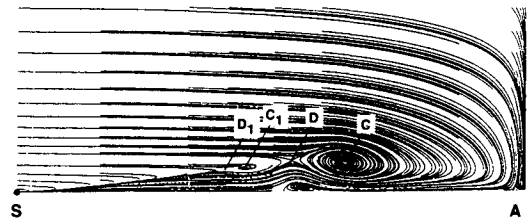

a) Particle traces in plane of symmetry

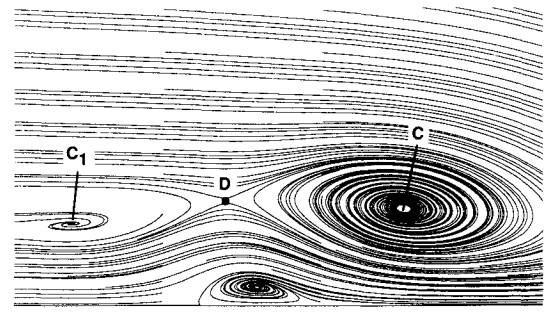

b) Details of secondary vortex

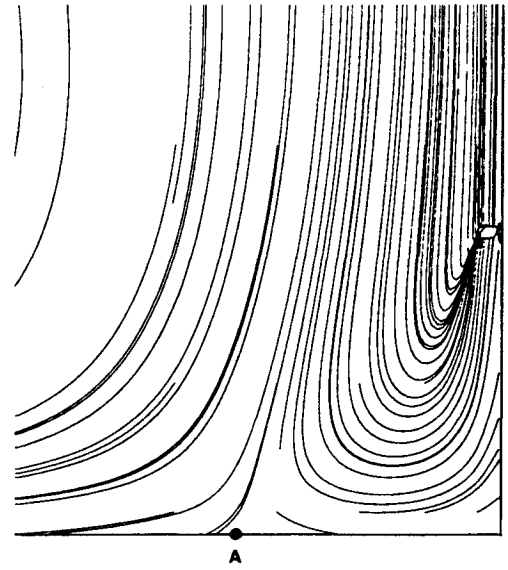

c) Detail of particle traces near the junction of cylinder and flat plate

Fig. 5 Results of a compressible code for $M_\infty = 0.2$, $Re_D = 1.5 \times 10^3$ wtih grid $103 \times 157 \times 35$.

lated oil-flow lines in the flat plate from results of code A with a grid system of $49 \times 97 \times 33$ for $Re_D = 1.5 \times 10^3$ and $\delta = 0.1D$ at 10 diam ahead of the cylinder. The grid used is quite different from that of Visbal's calculations. Figures 4a and 4b are results of code B with a grid of $103 \times 157 \times 35$ for Mach number 0.2 and $Re_D = 5 \times 10^2$, and Figs. 5a-c are results of code B for $Re_D = 1.5 \times 10^3$. These flow conditions and grid spacings are similar to those of Visbal's calculations. Whether Reynolds number, boundary-layer thickness, and number of grid points are similar to those of Visbal's calculations, or differ, the present results all confirm that the outermost singular point S is a saddle point of attachment. Therefore, we believe that the computed results have demonstrated the existence of saddle point attachment in the laminar flow before a protruded bluff body. We should note from the magnified plots of Figs. 3a and 5a (Figs. 3c and 5c) that there is no small secondary vortex near the juncture; the flow topology is also a saddle point of attachment on the cylinder near the juncture of cylinder with the plate. (In Fig. 5c, some grid resolution and graphic problems appeared near the saddle point of attachment on the cylinder.)

As Re_D increases to 1.5×10^3 in code B calculations, the primary horseshoe vortex evolves to 2 with a secondary separation in between (Figs. 5a and 5b). The secondary separation originates at a saddle point of separation. A geometry of a straight wing at zero incidence mounted on a flat plate was also calculated by code A for the same flow conditions as those used in Fig. 3, with a half-C grid of $97 \times 49 \times 49$. The wing geometry (Fig. 6a) is the same as that used in Ref. 7 for a turbulent flow. The laminar solution (Fig. 6b) also shows a saddle point of attachment with no spiral horseshoe vortex. From Figs. 6b, 4a, and 5a, the pattern evolves from one with no spiral horseshoe vortex, then with a single horseshoe vortex, and finally with multiple spiral horseshoe vortices.

Examining Fig. 11d of Ref. 16 carefully, one would speculate that the result of Kaul et al.[16] was also a saddle point of attachment, not a saddle point of separation. The data of Kaul et al. is unavailable, but a set of data of Rogers et al.,[17] where a similar computer code was used, is available. Figure 7 is a plot of particle traces in the plane of symmetry for a single post, simulated by Rogers et al.[17] The main singular point is very similar to a saddle point of attachment, except for some minor differences such as that the singular point is off, but very close to, the wall surface. (It is difficult to explain why the singular point of their result is off the wall surface. We experienced a similar feature in some of our solutions when they had not reached steady state.) There is also no spiral horseshoe vortex in the flow structure, very much like Fig. 6b. Therefore, we conjecture that a saddle point of attachment was obtained, but was not correctly interpreted, in some earlier laminar incompressible flow calculations.

This leads to an unanswered question: Under what conditions will the form of saddle point change from attachment to separation, or vice versa? So far the saddle point of attachment is observed only in cases of laminar flow. Previous calculations of turbulent supersonic flow past a blunt fin or incompressible turbulent flow for a juncture all exhibit a saddle point of separation, with a horseshoe vortex. In present

calculations for a turbulent case of $Re_D = 3.5 \times 10^5$ with $\delta = 0.2D$ at an upstream location of $10D$ (code A), the structure is also a saddle point of separation, similar to previous observations. Calculations for laminar subsonic cases of Mach number 0.6 and 2.0 with $Re_D = 1.5 \times 10^3$ and $\delta = 0.1D$ at an upstream location of $20D$ (code B) are being conducted to investigate the effect of compressibility. For the case of Mach number 0.6 (not shown here), the structure still contains a saddle point of attachment. For the case of Mach number 2.0, the flow involves a strong shock wave/boundary-layer interaction with the results that the outermost singular point on the surface moves far upstream to about $x/D = -6.9$, and the flow structure has evolved to one with complicated multiple horseshoe vortices. At first glance of Fig. 8a, the outermost singular point on the flat plate appears to have changed to a saddle point of separation. However, an enlargement (Fig. 8b) near the singular point shows that it remains a saddle point of attachment. (The details of its flow structure also indicate that the singular point on the cylinder remains a saddle point of attachment.) This is equivalent to the structure in Fig. 3 or 4, with the saddle point D very close to the outermost singular point S. As the two points approach each other, one can imagine that the question of grid resolution will become of crucial importance in determining the correct flow topology.

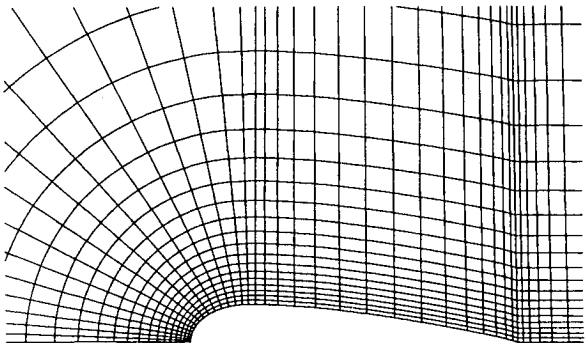

a) Wing geometry and grid system of $97 \times 49 \times 49$

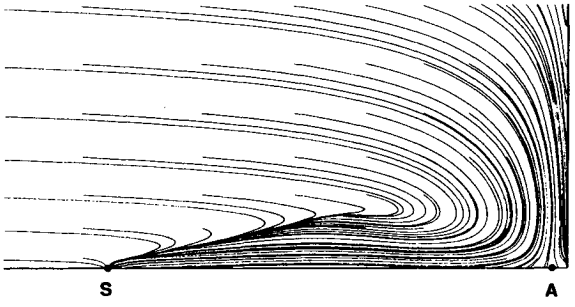

b) Particle traces in plane of symmetry

Fig. 6 Computation of a straight wing mounted on a flat plate for an incompressible flow of $Re_C = 1.5 \times 10^3$.

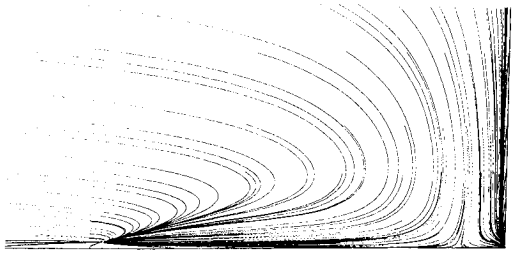

Fig. 7 Particle traces in plane of symmetry from results of Rogers et al.[17]

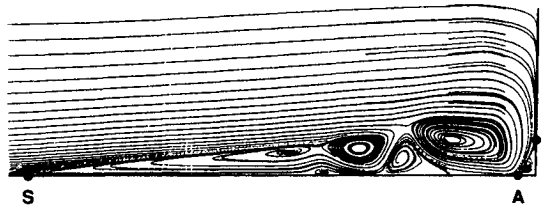

a) Particle traces in plane of symmetry

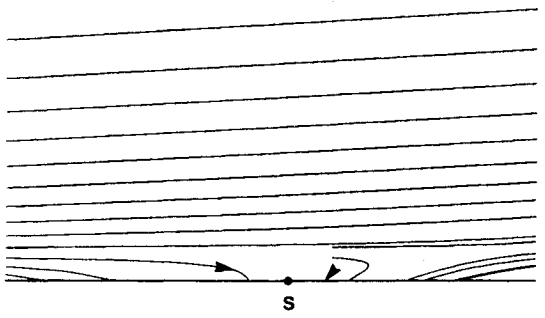

b) Details of flowfield near outermost singular point

Fig. 8 Results for $M_\infty = 2.0$, $Re_D = 1.5 \times 10^3$ wtih grid $103 \times 157 \times 35$.

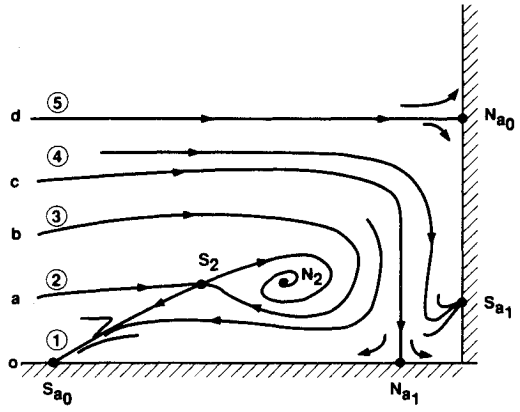

Fig. 9 Sketch of flow structure in plane of symmetry.

From these results, we can depict an evolution process of the change of flow structure. It becomes evident that the flow structure illustrated in Fig. 6 or 7 is the one that is fundamental to the encounter of a boundary layer with a bluff body protuberance. It is the first and simplest of a sequence and, at this initial stage, does not contain a spiral horseshoe vortex. The flow structure illustrated in Figs. 2–4 is the first structural change, and the flow structures of Fig. 5 or 8 are further structural changes to exhibit multiple spiral horseshoe vortices. The flow topology in the plane of symmetry of Figs. 2–4 can be summarized in a sketch (Fig. 9). In Fig. 9, S_2 and N_2 are a saddle point and spiral nodal point (a focus), respectively. There is no point of separation; all are points of attachment on the plate and cylinder—Sa_0 and Sa_1 saddle point of attachment, and Na_0 and Na_1 nodal points of attachment. Note that, topologically, the nodal point of attachment corresponding to Sa_0 is Na_0 on the cylinder, not point Na_1 on the plate. The nodal point of attachment Na_1 corresponds to the saddle point of attachment Sa_1 near the corner. The incoming fluid is divided into five distinct layers entraining into the various parts of the flow structure. It is of interest to note that, as saddle point S_2 moves closer to and merges with point S_0 on the surface, the flow topology will become the conventional one featuring a saddle point of separation. In other words, this is how the conventional horseshoe vortex separation before a protuberance can evolve from the flow with a saddle point of attachment illustrated in Fig. 9.

III. Theoretical Analysis

To set the stage for discussion, some theoretical analyses for flow near a singular point are summarized here. Interest will be focused on a singular point of the flat plate in the plane of symmetry. With higher-order terms neglected, the Taylor series expansion of the velocity about a singular point for limiting streamlines (or skin-friction lines) near/on the wall for incompressible flow is given as

$$\begin{aligned} uz^{-1} &= a_1x + b_1y + c_1z \\ vz^{-1} &= a_2x + b_2y + c_2z \\ wz^{-1} &= a_3x + b_3y + c_3z \end{aligned} \tag{1}$$

Here the origin of coordinate system (x, y, z) is set at a wall singular point. The solution curves for uz^{-1} and vz^{-1} in plane $z = 0$ of Eqs. (1) are identical with the skin-friction lines. Expressions (1) are substituted into the vorticity equation, the continuity equation, and the Navier-Stokes equations with only the first-order terms retained. For the present study, the flow is assumed symmetric with respect to y, and the equations become

$$\begin{bmatrix} uz^{-1} \\ vz^{-1} \\ wz^{-1} \end{bmatrix} = \begin{bmatrix} -a & 0 & c \\ 0 & b & 0 \\ 0 & 0 & \tfrac{1}{2}(a-b) \end{bmatrix} \begin{bmatrix} x \\ y \\ z \end{bmatrix} \tag{2}$$

Here, a, b, and c can be related to derivatives of vorticity and pressure at the critical point as

$$a = -\eta_x, \quad b = -\xi_y, \quad c = p_x/2\mu, \quad \tfrac{1}{2}(a-b) = p_z/2\mu$$

where ξ and η are the vorticity components in the x and y directions, respectively; $\nabla \times \boldsymbol{V} = \xi i + \eta j$; p and μ are the pressure and viscosity, respectively; and the subscripts denote partial differentiations.

The eigenvalues of this matrix are very simple. They all are real and equal to the three diagonal terms, respectively. The sum of the first two diagonal terms is equal to the negative of twice the third term. This indicates the fundamental property that the singular points in the three orthogonal planes, $(x\text{-}y)$, $(x\text{-}z)$, and $(y\text{-}z)$, cannot all be of one type; the singular points will be a combination of saddle and nodal points in the three planes. This ensures that parts of the flow will enter and other parts of the flow will leave the neighborhood of the singular point. From Eq. (2), the matrices in planes $(x\text{-}y)$ and $(y\text{-}z)$ are conical, and the matrix in plane $(x\text{-}z)$ has two eigenvectors

$$z = 0$$

$$\frac{z}{x} = \frac{(3a-b)}{2c}$$

This implies that flow separates or attaches from/to the wall at the singular point with an angle θ where $\tan\theta = (3a-b)/2c$. For the outermost singular point, we can expect that $a > 0$, $b > 0$, and the singular point is a saddle point in the $z = 0$ plane. Two cases are possible:

1) For $a > b > 0$, it will be a half saddle point in the $(x\text{-}z)$ plane and a half nodal point in the $(y\text{-}z)$ plane. The fluid leaves the surface $(z = 0)$ and, hence, the singular point is a saddle point of separation.

2) For $b > a > 0$, it will be a half nodal point in the $(x\text{-}z)$ plane and a half saddle point in the $(y\text{-}z)$ plane. The fluid enters the singular point and, hence, the singular point is a saddle point of attachment.

Presence of the so-called saddle point of separation or attachment is based on the fact that the critical point is a saddle point in the wall surface, and the fluid is entering (attachment) or leaving from (separation) the singular point on the wall. Since $\frac{1}{2}(a-b) = p_z/2\mu$, attachment points indicate a pressure decrease and separation points indicate a pressure increase in the direction away from the wall $(z = 0)$.

Another case of interest occurs when $a \cdot b < 0$. The singular point is a nodal point in the $(x\text{-}y)$ plane and half saddle in both $(x\text{-}y)$ and $(y\text{-}z)$ planes. There are two possible circumstances:

1) For $a > 0$, $b < 0$, so that $\frac{1}{2}(a-b) > 0$, the flow leaves the singular point and the singularity is a nodal point of separation.

2) For $a < 0$, $b > 0$, so that $\frac{1}{2}(a-b) < 0$, the flow enters the singular point and the singularity is a nodal point of attachment. The singular point A in Figs. 2–5 belongs to this case.

Similarly, presence of a nodal point of separation or attachment is based on the fact that the singular point is a nodal point on the wall surface, and the fluid is entering or leaving the singular point. If the eigenvalues in the $(x\text{-}y)$ plane are the same and equal, i.e., $a = -b$, the singular point is a proper node, and if not, it is an improper node.

As obtained from the above, the three-dimensional singular point always consists of one nodal and two saddle points in three planes $(x\text{-}y)$, $(x\text{-}z)$, and $(y\text{-}z)$, respectively. The unique characteristic of a nodal point (half or full) is that there is an infinite number of streamlines, or trajectories, that enter into or emanate from the point such that these streamlines make up a surface. For the saddle point of separation, the half nodal point is in the $(y\text{-}z)$ plane and the streamlines in the $(y\text{-}z)$ plane, which form the new stream surface, leave the critical point in two possible ways (as shown in Fig. 10). For $3b > a > b$, all of the streamlines are tangent to the z axis (Fig. 10a), and for $a > 3b$, all of the streamlines are tangent to the y axis (Fig. 10b). (Here, y and z are principle axes.) In other words, the new stream surface in the $(x\text{-}y)$ plane is attached to a pair of skin-friction lines emanating away from the singular point. In the $(x\text{-}z)$ plane, the separation streamline will leave the singular point on the wall surface at an angle θ where $\tan\theta = (3a-b)/2c$. The value of c is greater than zero for both saddle point of separation and attachment (as will be discussed later). Since $a > b$ for the separation case, the inclination angle of eigenvector $(z/x) = (3a-b)/2c$ is less than 90 deg. For the attachment case, the half nodal point is in the $(x\text{-}z)$ plane, and so is the associated stream surface. For the present case, the attachment angle is less than 90 deg and, hence, $3a > b > a$. This also implies that all of the streamlines in the $(x\text{-}z)$ plane enter the singular point at an angle θ where $\tan\theta = (3a-b)/2c > 0$, i.e., $\theta < 90$ deg. For the case of $3a < b$, $\theta > 90$ deg and all streamlines in the $(x\text{-}z)$ plane, except the eigenvector, will enter the singular point tangent to the other eigenvector, $z = 0$.

For incompressible flows, as pointed out by Tobak,[17] there is a pressure extremum associated with each critical point on the wall. For the present study, along the line of symmetry, there is a pressure minimum ahead of a saddle point, either separation or attachment, and a pressure maximum behind the nodal point of attachment. As discussed in the previous section, the corresponding saddle point of attachment for nodal point A is on the cylinder near the juncture with the flat plate, not the outermost singular point S. These make the pressure gradient term in Eq. (2) $c = p_x/2\mu > 0$ at saddle point S, and $c < 0$ at nodal point of attachment A.

Now we evaluate the magnitude of three parameters a, b, and c from the computed results to determine the characteris-

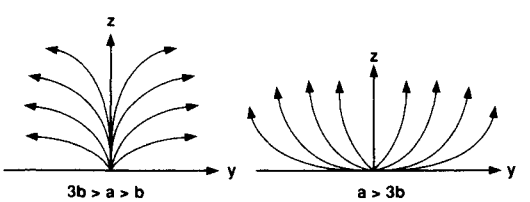

Fig. 10 Two possible streamline patterns in $(y\text{-}z)$ plane for a saddle point of separation.

tics of the critical point and the attachment angle. A first-order-difference scheme is used to evaluate the parameters a, b, and c. For the case of Fig. 3, $a = 2.76$, $b = 3.34$, $c = 24.5$ and results in that $a/b = 0.83$ and $\theta = 5.86$, which is consistent with the plotted particle traces in Fig. 3. The saddle point of attachment is located at $x/D = -2.03$ and a corresponding pressure minimum is obtained ahead of S, at about $x/D = -7.15$. For the case of Fig. 4 for code B, $a = 0.966$, $b = 1.229$, $c = 6.289$ and results in $a/b = 0.786$ and $\theta = 7.56$, which is consistent with the plotted particle traces in Fig. 4. The saddle point of attachment is located at $x/D = -2.38$, and a corresponding pressure minimum is obtained ahead of S, at about $x/D = -8.54$. The location of the pressure minimum is far ahead of the saddle point of attachment S and is in a region with very small pressure variation. Therefore, it is difficult to locate the position accurately. In all of the present calculations, the attachment angle varys roughly between 5.0 and 10.5 deg.

The analysis can also apply to the nodal point of attachment A. For the case of Fig. 3, $a = -281$, $b = 177$, $c = -118$, and results in $\theta = 76.94$. The nodal point of attachment A is located at $x/D = -0.541$, and a corresponding pressure maximum is obtained at about $x/D = -0.545$. For the case of Fig. 4 for code B, $a = -109$, $b = 62.3$, $c = -39.63$, and results in $\theta = 78.5$. The nodal point of attachment A is located at $x/D = -0.568$, and a corresponding pressure maximum is obtained at about $x/D = -0.575$. Note that the attachment angle for the nodal point of attachment A is very large and its corresponding pressure maximum is located very close to the singular point itself.

IV. Discussion

A. External Flow Structure

Our first concern is the construction and understanding of the external flow structure for flow upstream of a protruded bluff body. It has been known for a long time that, given a surface flow pattern, an external flow structure that could be constructed from it may not be unique. However, it has been generally assumed that circumstances would decide which of the possible alternatives would be the one correct structure that fit the circumstances. Here, there can be at least two structures that fit the circumstances. Based on the numerical results in Sec. II and theoretical analysis in Sec. III, a same surface skin-friction pattern before an obstacle can have two very different external flow structures: One is a case of separation, as conventionally conceived (Fig. 1), and another is a case of attachment, as sketched in Fig. 11. The one chosen by the flow is determined by the particular values of the geometric and flow parameters in play. This should make us cautious in the construction of external flows on the basis of surface flow patterns alone. Clearly, it is important to have in hand information about the external flow that would enable us to choose between alternative constructions.

It is of interest to understand the similarities and differences between the two structures, Figs. 1 and 11. In Fig. 1, there is a stream surface, originating in the transverse plane, that is new and unique. All of the streamlines forming that surface emanate from a half node lying in the surface at the juncture with the saddle point in the surface flow pattern and do not come from upstream or somewhere else. The stream surface forms a barrier and the neighboring fluid in the boundary layer must go upward and spiral around the surface. Therefore, we have called it a separation surface. For the attachment case (Fig. 11), there is again a nodal point, in the (y-z) plane, that generates a surface but now it is in the flow and becomes a full node. (In Fig. 1, the singular point is a half saddle in the plane of symmetry, and in Fig. 11, it is a full saddle, as S_2 in Fig. 9.) Note that the new surface also acts as a barrier to the oncoming flow, just as in the case of separation. Nevertheless, the corresponding singular point on the wall is now a saddle point of attachment and the flow behavior near it is quite different from that near the saddle point of separation, as discussed in the previous section. In Fig. 11, the full nodal point generates a stream surface with two distinct parts. One part of the stream surface, the upper part, behaves like the separation surface of Fig. 1 in that the streamlines making up surface spiral into the horseshoe vortex. The other part of the stream surface, the lower part, attaches to the pair of skin-friction lines emanating outward from the saddle point of attachment. In essence, the difference between Figs. 1 and 11 is the existence of the lower part of the stream surface in Fig. 11. When the full nodal point moves to the wall and becomes a half node, the lower part of the stream surface disappears and, hence, Fig. 11 becomes the same as Fig. 1. Nevertheless, with respect to the flow near the wall, the flow near the lower part of the stream surface in Fig. 11 is quite different from that near the separation surface of Fig. 1. It is this situation that calls for special attention to be directed to the interpretation of surface oil-streak lines.

B. Oil-Accumulation Line

In the conventional terminology, when a limiting streamline exists toward which adjacent limiting streamlines converge from both sides, it is called a line of separation. Equivalently, in an experiment, an oil-streak line toward which adjacent oil-streak lines converge from both sides will be interpreted as a line of separation in an oil-flow pattern. Likewise, it is conventionally accepted that a necessary condition for presence of a line of attachment is that it be a line away from which adjacent lines (limiting streamlines or oil streaks) diverge on both sides.

Should a saddle point of attachment be present, interpretations of the oil-flow pattern and topology are not that straightforward. Without examining the properties of the singular point in other planes, a line of oil accumulation or a skin-friction line emanating outward from a saddle point cannot be simply interpreted as a line of separation. As demonstrated in Figs. 3–5, critical point S is a saddle point of attachment, and the half-node is in the (x-z) plane. Hence, so is its associated stream surface, as discussed in the theoretical analysis of Sec. III. Thus, the skin-friction line S-P in the plane (x-y) that is emanating from the saddle point of attachment S does not form the base of a stream surface of separation, even though adjacent skin-friction lines are converging from both sides to the line S-P. (As discussed in connection with Fig. 11, there is a part of a stream surface, the lower part, generated from a full node that attaches to the line S-P, but it is in a sense of attachment rather than separation.) This implies that fluid adjacent to line S-P has no sense of separation from the wall surface and, hence, it becomes misleading to call line S-P a line of separation. Since it is a particular line associated with an attachment point, and its surrounding fluid has some sense of attachment, it would be more meaningful to call line S-P a line of attachment (see later for definition). Now, even though the flow exhibits features of a spiral horseshoe vortex and

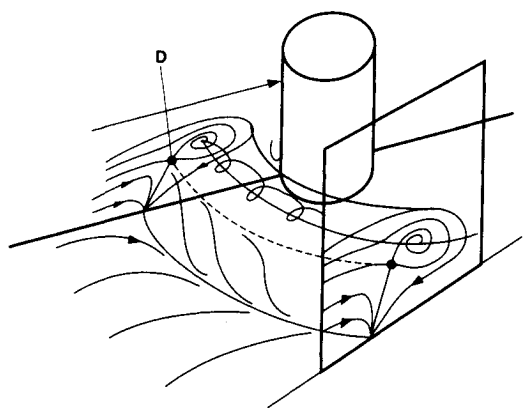

Fig. 11 Alternative external flow structure system of a cylinder mounted on a flat plate.

several singular points, should we classify both *S-P* and *A-B* as lines of attachment, then in Figs. 3b and 4b, there is no line of separation on the flat plate. Similarly, on the basis of this classification, it would no longer be a necessary condition that a line of attachment show evidence of the divergence of oil streaks from both sides of the line. The question now is, What are the proper definitions of a line of separation and a line of attachment?

C. Line of Separation

A three-dimensional separation can be classified in various ways. In the present study, we consider only the case of regular separation or attachment; i.e., as Lighthill[11] and Legendre[19] suggested, separation and attachment are associated with singular points in a skin-friction line pattern.

Following the previous discussion, we now see that it can be misleading to call a line emanating outward from a saddle point a line of separation purely on the basis of observing only the pattern of skin-friction lines on the wall surface. Observation of the state of the external flow is required as well. The saddle point has to be a saddle point of separation. Only if the line is a skin-friction line emanating from a saddle point of separation should it be called a line of separation. As discussed in Sec. III, there is a new unique stream surface, called a separation surface, composed of streamlines emanating away from the critical point, and the line of separation is the trace of the junction of that unique separation surface with the wall surface. Topologically, based on the criterion that a saddle-to-saddle connection is structural unstable (cf. Chapman[13]), a line of separation, originating from a saddle point of separation, ultimately will connect to a nodal point or a spiral focus of separation. Hence, the separation surface will not reattach to the wall (forming a totally closed bubble); instead, it will spiral into a vortex.

In light of this, we can speculate that previous instances may exist where the interpretation of oil-flow patterns alone may have led to the erroneous conclusion that flow separation was present. All such cases need careful re-examination, in which the state of external flow must be taken into account.

D. Line of Attachment

Attachment and separation are two main features of skin-friction line or oil-flow patterns in a study of three-dimensional separation. In high-speed flow, the neighborhood of the attachment point (or line) is often associated with high pressure and peak heating, and actually is of great concern to design engineers. Nevertheless, previous studies of three-dimensional flow separation tend to emphasize the definition of line of separation and pay less attention to the definition of line of attachment. There has never been any mathematical study of its associated behavior and characteristics. Very often an attachment process has been simply treated as the reverse process of separation.[19] From the previous discussion, one can clearly see that, except for some simple flow structures, an attachment process is not the reverse of the separation process.

Historically, the line of attachment has never been well defined. Conventionally, except at a leading edge, it is identified on the basis of two features: 1) divergence of skin-friction lines as a necessary condition, and 2) counter to but paired with a line of separation. These two features are based more on appearance than on theoretical analysis. The criterion of the divergence of skin-friction lines is ambiguous. Based on linear analysis, all skin-friction lines emanating from a node of attachment are divergent from each other at the origin. Moreover, even if they start divergent from each other, farther downstream they may change and begin to converge apparently to form a line that ends at a nodal point of separation, or a spiral (focus) of separation. Now with the existence of a saddle point of attachment, both criteria become at least questionable and, in many circumstances, misleading.

Recognizing the difficulty of establishing an unambiguous definition for a line of attachment, we propose the following redefinition as an attempt to take into account the new cir-

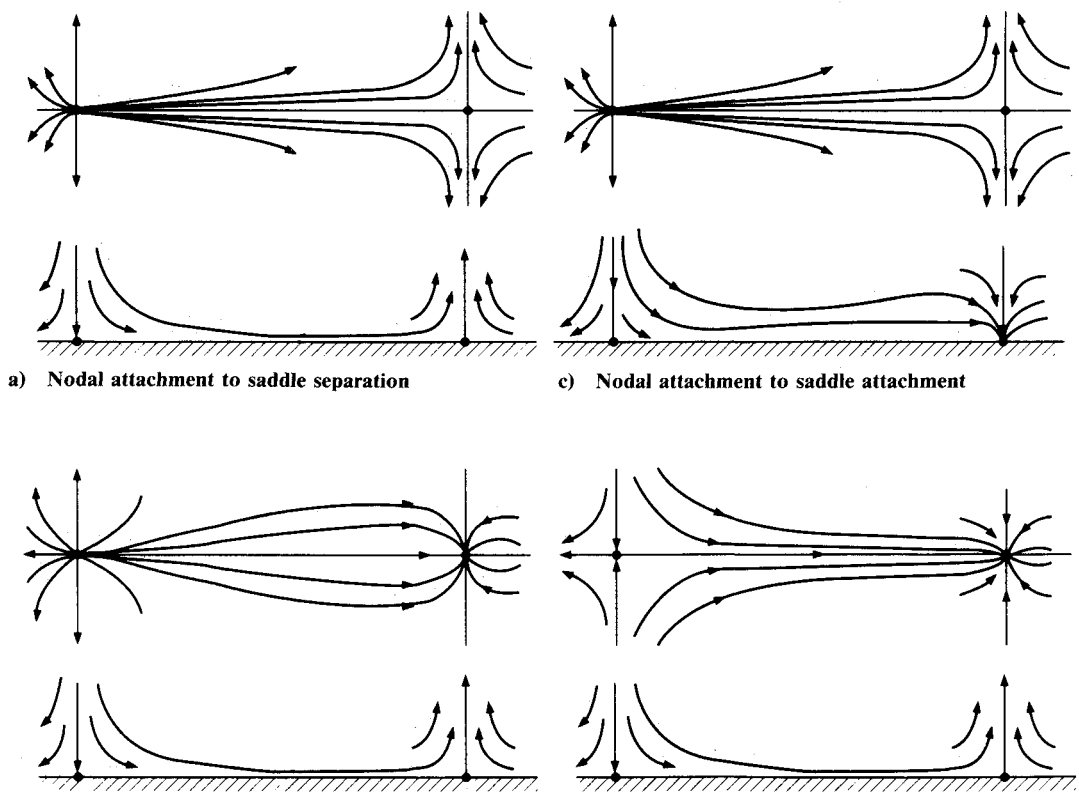

a) Nodal attachment to saddle separation

c) Nodal attachment to saddle attachment

b) Nodal attachment to nodal separation

d) Saddle attachment to nodal separation

Fig. 12 Four possible connections of line attachment.

cumstances brought to light by the existence of the saddle point of attachment: A line of attachment is defined as a skin-friction line emanating outward either from a saddle point of attachment or a nodal point of attachment and having the property of dividing its surrounding flow topology into two definable sets or groups. Here, sets can be singular points or geometries. The division of the flow topology can be caused by any of a number of reasons, e.g., fulfillment of symmetry conditions or existence of multiple sinks (i.e., nodal points of separation) where adjacent sets of skin-friction lines may have different endpoints. There will be only two lines of attachment emanating outward from a saddle point of attachment. However, there can be many lines of attachment emanating from a nodal point of attachment, depending on flow conditions and geometry. Based on this definition, in Figs. 3b and 4b, *A-S, A-B, A-E,* and *S-P* all are lines of attachment. Their common features are that 1) adjacent fluid moves downward toward the wall near their corresponding critical point, and 2) they divide their surrounding flow pattern into two groups. For example, line *S-P* divides the skin-friction lines from a nodal point upstream and from nodal point *A*. Lines *A-S* and *A-E* divide the flow pattern symmetrically.

A line of attachment may connect to various kinds of singular points. Figures 12a–d show, for the sake of discussion, conceptually simplified sketches of four possible connections. A line of attachment from a nodal point of attachment can terminate at a nodal point of separation (Fig. 12b), a saddle point of separation (Fig. 12a), and a saddle point of attachment (Fig. 12c). Based on the concept that a saddle-to-saddle connection is structurally unstable, a line of attachment from a saddle point of attachment can only terminate at a nodal point of separation (Fig. 12d). (Here, case of spiral separation is implied as a node of separation.) With connection of a nodal point of attachment to a saddle point of attachment, the sense of the external flow structure remains the same throughout. With connection of a nodal (saddle) point of attachment to a saddle (nodal) point of separation, the flow structure changes from an appearance of attachment to one of separation. In other words, the sense of the fluid adjacent to a line of attachment will be toward the wall near the critical point of attachment, but the sense will change to be upward away from the wall surface as sketched in Figs. 12a, 12b, and 12d. This is quite different from a line of separation. A line of separation, emanating from a saddle point of separation, will connect to a nodal point of separation. The fluid adjacent to the line of separation, starting with a sense of moving away from the surface, will keep the same sense throughout.

E. Convergence of Skin-Friction Lines and Acceleration

Another interesting point associated with a saddle point of attachment is the presence of flow acceleration even though adjacent skin-friction lines are convergent. Assuming the flow is incompressible, the mass-flow relation is, as derived by Lighthill,[11]

$$\tfrac{1}{2}\omega_w z^2 b = c \tag{3}$$

where c is the volume flow along the limiting streamtube, ω_w the magnitude of vorticity at the surface, z the height, and b the distance between two adjacent skin-friction lines. It is conventionally considered that stream tubes can greatly increase their distance from the surface either by ω_w becoming small or by skin-friction lines running very close together. That is the concept of separation. In the case of a saddle point of attachment, it becomes apparent that, as the distance of streamlines from the surface decrease and the skin-friction lines converge, in order to preserve a constant mass flow ω_w must increase; i.e., the flow speeds up, in contrast to the case of separation in which the flow slows down.

Near the surface, a velocity is strongly affected by friction or viscosity and, hence, cannot continually increase to balance the decrease of b and z in Eq. (3) for a saddle point of attachment. Thus, there results a subtle but fundamental difference between the appearances of a saddle point of attachment and of separation. The degree of convergence to a line of attachment originating from the saddle point is substantially weaker than it is for a line of separation. This is observed from computed results and also can be confirmed from the previous analysis.

V. Conclusions

Low-speed flows over a cylinder mounted on a flat plate have been numerically studied. The Navier-Stokes equations were solved by an incompressible code and a compressible code for a range of Reynolds numbers, grid spacings, and number of grid points. The results have shown that the outermost singular point on the flat plate is a saddle point of attachment for laminar flow. In contrast, it is a saddle point of separation for the turbulent case. (Previous results for blunt fins and wing junctures have also shown that it is a saddle point of separation for turbulent cases.) Calculations for laminar flows of Mach number 0.6 and 2.0 have been conducted to investigate the effect of compressibility. The outermost saddle point for Mach number 0.6 or 2.0 remains a saddle point of attachment. However, for the case of Mach number 2.0, the singular point that separates the spiral vortex (or vortices) and the saddle of attachment now moves very close to the saddle point of attachment and, therefore, the structure of conventional spiral separation becomes the dominant feature. The computational results near the critical point have been theoretically analyzed. For the turbulent case, the ratio of vorticity gradients in the x and y directions is $\eta_x/\xi_y > 1$, and the singular point is a saddle point of separation. For the laminar case, $\eta_x/\xi_y < 1$, and the singular point is a saddle point of attachment.

The significance of the saddle point of attachment to the construction of external flow structures, the interpretation of experimental surface oil-flow patterns, and the theoretical definition of three-dimensional line of separation have been discussed. The potential presence of a saddle point of attachment means that a line of oil accumulation from both sides of a skin-friction line emanating outward from a saddle point can be either a line of separation or a line of attachment. By the same token, flow adjacent to a line of attachment can be either divergent from or convergent to both sides, depending on the characteristic of the attachment point. A precise definition of the line of separation has been re-established: It is the line originating from a saddle point of separation. We have proposed defining the line of attachment as a skin-friction line emanating outward from a critical point of attachment that divides the surrounding flow topology into two definable sets or groups. We also note that fluid adjacent to a line of attachment, starting in a sense of fluid flowing toward the wall near the critical point of attachment, may change to a sense of flowing upward away from the wall. This is quite different from the fluid adjacent to a line of separation, which always has the same sense of flowing away from the wall.

Acknowledgment

The first author is deeply indebted to Murray Tobak for his many valuable comments and intriguing discussions.

References

[1]Thwaites, B. (ed.), *Incompressible Aero-Dynamics,* Oxford Univ. Press, Oxford, England, UK, 1960, pp. 551–554.

[2]Baker, C. J., "The Laminar Horseshoe Vortex," *Journal of Fluid Mechanics,* Vol. 95, Pt. 2, 1979, pp. 347–367.

[3]Eckerle, W. A., and Langston, L. S., "Horseshoe Vortex Formation Around Cylinder," *ASME Journal of Turbomachinery,* Vol. 109, No. 2, 1987, pp. 278–289.

[4]Sedney, R., and Kitchens, C. W., Jr., "The Structure of Three-Dimensional Flows in Obstacle-Boundary Layer Interaction," *Flow Separation,* AGARD CP-168, Paper 37, 1975.

[5]Dolling, D. S., and Bogdonoff, S. M., "Blunt Fin-Induced Shock

Wave/Turbulent Boundary Layer Interaction," *AIAA Journal,* Vol. 20, No. 12, 1982, pp. 1674–1680.

[6]Hung, C. M., and Buning, P. G., "Simulation of Blunt-Fin-Induced Shock Wave and Turbulent Boundary-Layer Interaction," *Journal of Fluid Mechanics,* Vol. 154, May 1985, pp. 163–185.

[7]Sung, C. H., "An Explicit Runge-Kutta Method for 3-D Turbulent Incompressible Flows," David Taylor Naval Ship Research Center, Rept. DTNSRDC/SHD-12441-01, Bethesda, MD, July 1987.

[8]Shang, J. S., McMaster, D. L., Scaggs, N., and Buck, M., "Interaction of Jet in Hypersonic Cross Stream," *AIAA Journal,* Vol. 27, No. 3, 1989, pp. 323–329.

[9]Visbal, M. R., "Numerical Investigation of Laminar Juncture Flows," AIAA Paper 89-1873, June 1989.

[10]Visbal, M. R., "On the Structure of Laminar Juncture Flows," *AIAA Journal,* Vol. 29, No. 8, 1991, pp. 1273–1282.

[11]Lighthill, M. J., "Attachment and Separation in Three-Dimensional Flow," *Laminar Boundary Layers,* edited by L. Rosenhead, Oxford Univ. Press, Oxford, England, UK, 1963, pp. 72–82.

[12]Davey, A., "Boundary-Layer Flow at a Saddle Point of Attachment," *Journal of Fluid Mechanics,* Vol. 10, Pt. 4, 1961, pp. 593–610.

[13]Chapman, G. T., "Topological Classification of Flow Separation on Three-Dimensional Bodies," AIAA Paper 86-0485, Jan. 1986.

[14]Perry, A. E., and Fairlie, B. D., "Critical Points in Flow Patterns," *Advances in Geophysics,* Vol. 18B, 1974, pp. 299–315.

[15]Chakravarthy, B. R., Szema, K. Y., Goldberg, U., Gorski, J. J., and Osher, S., "Application of a New Class of High Accuracy TVD Scheme to the Navier-Stokes Equations," AIAA Paper 85-0165, Jan. 1985.

[16]Kaul, U. K., Kwak, D., and Wagner, G., "A Computational Study of Saddle Point of Separation and Horseshoe Vortex Systems," AIAA Paper 85-0182, Jan. 1985.

[17]Rogers, S. E., Kwak, D., and Kaul, U. K., "A Numerical Study of Three-Dimensional Incompressible Flow Around Multiple Posts," AIAA Paper 86-0353, Jan. 1986.

[18]Tobak, M., private communication, 1990.

[19]Legendre, R., "Regular or Catastrophic Evolution of Steady Flows Depending on Parameters," *La Recherche Aerospatiale,* No. 1982-4, 1982, pp. 41–49.

[20]Zhang, H., "The Separation Criteria and Flow Behavior for Three-Dimensional Steady Separated Flow," *ACTA Aerodynamica Sinica* (translation), No. 1, 1985, pp. 1–12.